UNIVERSITY OF GLASGOW

PARTICLE PHYSICS EXPERIMENTAL

Third Year Ph.D Progress Report

Author:
Stephen OGILVY

Supervisors:
Dr. Lars EKLUND
Dr. Paul SOLER

May 3, 2013

Abstract

The track based software alignment of the LHCb experiment's Vertex Locator is susceptible to certain "weak modes" of misalignment which can bias physics relevant quantities. Work to investigate and mitigate this effect within the alignment software is outlined. Work is also detailed on an analysis to measure the $\Lambda_c^+ \to p^+h^-h^+$ ($h = K/\pi$) branching fractions ($\mathcal{BF}$s) using $1fb^{-1}$ of LHCb 2011 data at $\sqrt{s} = 7TeV$.

Contents

1 Introduction

1.1 The LHCb Experiment and VELO Detector

The LHCb experiment at CERN has been designed to make precision measurements in heavy flavour physics at never-before explored centre of mass energies. In 2012 it recorded data at a record-breaking $E_{CM} = 8\ TeV$ and gathered over $2fb^{-1}$ of data, having run throughout 2011 at $E_{CM} = 7\ TeV$ while collecting $1.04fb^{-1}$ of analysis-quality data. This has proven large enough to make a variety of world-best measurements of Standard Model quantities. Over the course of the LHCb's 20 year lifetime it will continually refine SM measurements, most notably the CKM Matrix elements governing the mixing of quark flavour states, put tighter constraints on the phenomena of charge-parity violation (CPV) and search for new physics and undiscovered particles. Glasgow's PPE group is involved with a variety of physics analyses in the charm and bottom sectors, including searches for CPV in the neutral D and B meson systems, lifetime measurements and searches for unobserved charmed baryons and excited B mesons.

Key to the LHCb physics programme is the silicon microstrip VErtex LOcator (VELO), which locates primary interaction and decay vertices and enables the accurate measurements concerning the long-lived heavy flavour particles of interest to LHCb physics analyses. The alignment of the LHCb detectors is crucial, and in order to ensure high performance of the VELO a rigorous alignment strategy has been implemented, involving initial optical surveys and software alignment algorithms for on-and-offline use, which utilise measurements of track residuals (the difference between the measured position of a sensor hit and the intercept with the sensor plane of the fitted track) to calculate misalignments. These software methods used employ a global χ^2 minimisation, an approach which despite its general utility is insensitive to specific forms of misalignment which leave the track χ^2 invariant. These are termed "weak modes" of misalignment. For VELO alignment a Kalman Filter is being utilised to constrain the weak modes, following on a MC study of weak mode effects on physics-relevant quantities previously performed by the author.

1.2 Charm Spectroscopy and Λ_c^+

The Λ_c^+ is a baryon containing a charm, down and up quark. Its most common hadronic decays are via $\Lambda_c^+ \to p^+h^-h^+$, where h is any combination of kaons and pions. The measured branching ratios as given by the PDG [1] are shown in Table 1. Of particular note is the doubly Cabibbo-suppressed mode $\Lambda_c^+ \to p^+\pi^-K^+$, which has not yet been observed. Current measurements constrain the decay's branching fraction to $< 2.3 \times 10^{-4}$ @ 90% CL.

Decay Mode	**PDG Branching Fraction**
$\Lambda_c^+ \to p^+K^-\pi^+$ (CF)	0.05 ± 0.013
$\Lambda_c^+ \to p^+K^-K^+$ (SCS)	$(7.7 \pm 3.5) \times 10^{-4}$
$\Lambda_c^+ \to p^+\pi^-\pi^+$ (SCS)	$(3.5 \pm 2.0) \times 10^{-3}$
$\Lambda_c^+ \to p^+\pi^-K^+$ (DCS)	$< 2.3 \times 10^{-4}$@90% CL

Table 1: The $\Lambda_c^+ \to p^+h^-h^+$ decay modes and their branching fractions.

2 Status of Research

2.1 VELO Weak Modes

The software alignment in LHCb uses a global track χ^2 minimisation approach. This is powerful but can be subject to forms of misalignment that leave the track χ^2 invariant; these forms of misalignment are called weak modes. These are poorly constrained statistically and are of concern in track-based alignment approaches because they can bias physics-relevant quantities while leaving quantities used in alignment invariant. In the VELO module alignment there are a variety of possible weak modes, as demonstrated in Figure 4.

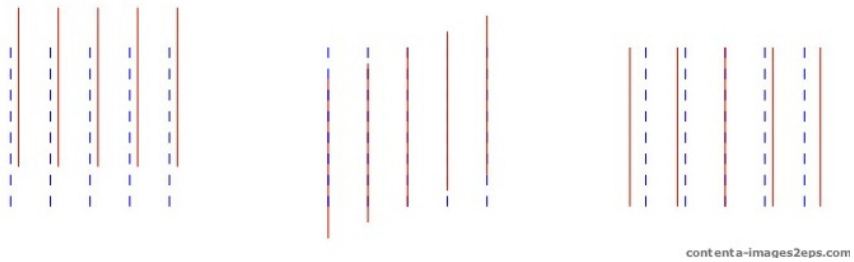

Figure 1: Weak modes of misalignment. Dashed blue lines show nominal module position, red lines show weak mode displacement. Shown left to right are overall translation, shearing and scaling. Reproduced from [2].

In the 2010 data a bias in the track $IP_{x/y}$ was observed, which is possibly caused by weak mode effects. This motivated an MC study on the effects of weak modes on the VELO track reconstruction, carried out by the author in their first year year, in order to investigate other potential biases and effects on alignment quantities. It was found that certain weak modes, specifically twists around z and shearing in x/y, can leave the track χ^2 invariant while introducing biases into physics-relevant quantities such as IPs. Notably a twist simulated with a magnitude small enough $(2\ \mu rad$ per module z position in mm) to leave the track χ^2 invariant created a bias in $IP_{x/y}$ which closely resembled such a bias observed in the 2010 data tracks. The IP_y distributions from data and the simulated twist are shown in Figure 5. The twist was found to be the dominant weak mode. As such it was decided to implement a configuration of the Kalman filter which would attempt to constrain these VELO weak modes. Work in investigating possible constraints and their effects on suppressing the weak modes is currently underway.

2.2 Measurement of Λ_c^+ $\mathcal{BF}$s

It is the aim of the analysis to measure the $\Lambda_c^+ \to p^+h^-h^+(h = K/\pi)$ branching fractions and attempt a first observation of the doubly Cabibbo-suppressed mode $\Lambda_c^+ \to p^+\pi^-K^+$. The branching fractions of the singly and doubly Cabibbo suppressed modes are measured relative to the cabibbo favoured $\Lambda_c^+ \to p^+K^-\pi^+$mode. The intermediate $\phi(1020)$ resonance in $\Lambda_c^+ \to p^+K^-K^+$ is also

isolated and measured relative to $\Lambda_c^+ \to p^+K^-\pi^+$. The ratios measured in the analysis are defined in (2.1).

$$\frac{\mathcal{BF}_{\Lambda_c^+\to p^+K^-K^+}}{\mathcal{BF}_{\Lambda_c^+\to p^+K^-\pi^+}}, \frac{\mathcal{BF}_{\Lambda_c^+\to p^+\pi^-\pi^+}}{\mathcal{BF}_{\Lambda_c^+\to p^+K^-\pi^+}}, \frac{\mathcal{BF}_{\Lambda_c^+\to p^+\pi^-K^+}}{\mathcal{BF}_{\Lambda_c^+\to p^+K^-\pi^+}}, \frac{\mathcal{BF}_{\Lambda_c^+\to p^+(\phi\to K^+K^-)}}{\mathcal{BF}_{\Lambda_c^+\to p^+K^-\pi^+}} \tag{2.1}$$

The analysis uses two sources of Λ_c^+ production: those produced directly from the proton-proton collision (prompt) and those from semileptonic $\Lambda_b^0 \to \Lambda_c^+\mu^-\bar{\nu}$ decays. The topology of these decays is ilustrated in Figure 2. The analysis lacks a suitable decay mode which mimics the characteristics of $\Lambda_c^+ \to p^+h^-h^+$ decays to act as a cross check. In place of this independent measurements are made with the prompt and semileptonically produced samples, and until agreement between these two samples can be established the unobserved $\Lambda_c^+ \to p^+\pi^-K^+$ mode will be kept blind.

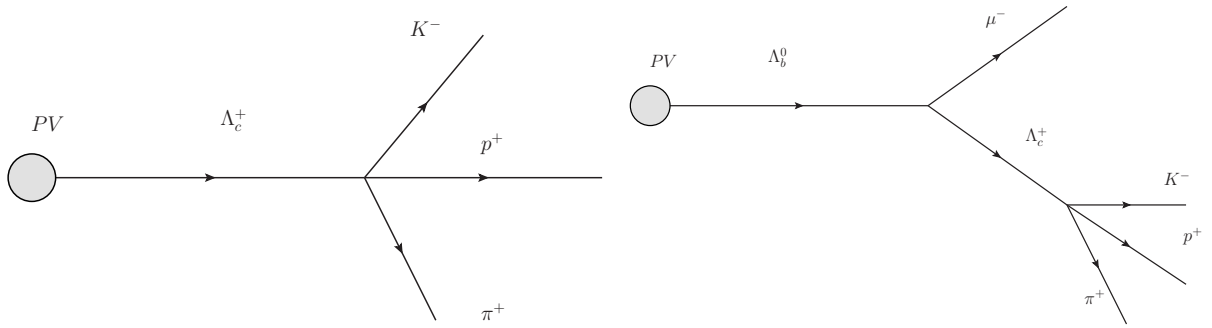

(a) Prompt

(b) Semileptonic

Figure 2: The topologies of the two sources of Λ_c^+ decays used in the analysis.

2.2.1 Data Selection

The selection of interesting events takes place over numerous stages. Most of the 40m p-p collisions taking place in the detector are of no interest to physics analyses. The LHCb hardware trigger partially reconstructs each event, selecting those of interest with a number of criteria, for example the highest transverse energy (E_T) hadron, electron and photon clusters in the calorimeters. The event rate is cut to 1MHZ and these events are then processed by the software trigger, which then reconstructs the full event and employs kinematic cuts to further reduce the overall output rate to 5kHZ, which is stored on tape.

The data on tape is then processed centrally in a procedure referred to as "stripping", whereby events of certain types are grouped together for use in physics analyses. At this level further kinematic cuts are employed to reject background events. There exist separate trigger and stripping algorithms for the treatment of the prompt and semileptonic samples. One further refinement of the data is performed offline for enhancement of signal/background discrimination. In the prompt sample to suppress the high combinatoric background we employ a boosted decision tree to select events. In the semileptonic sample the greater separation of the Λ_c^+ from the primary vertex results in a much lower combinatoric background than in the prompt sample, and minimal vertex quality

cuts are sufficient to maximise the discrimination between signal and background. The final mass fits for the prompt and semileptonic $\Lambda_c^+ \to p^+K^-\pi^+$ decays are shown in figure 3, and illustrate the high statistics available to the analysis.

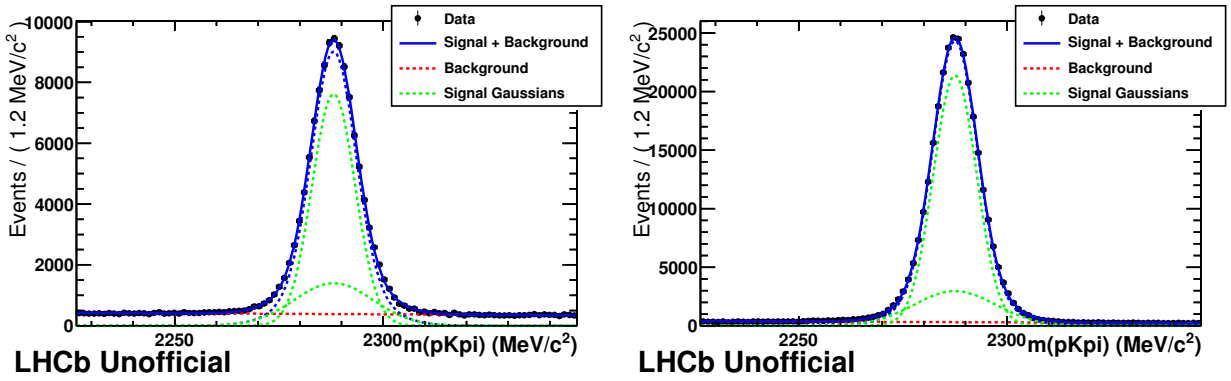

(a) Prompt

(b) Semileptonic

Figure 3: The topologies of the two sources of Λ_c^+ decays used in the analysis.

2.2.2 Evaluation of Efficiencies

The efficiencies of our selection on the various decay modes must be taken into account. These may be factorised into the efficiency of the trigger, the stripping and the offline selection. The efficiency of the trigger and stripping is evaluated using simulated Monte Carlo (MC) data. The offline efficiency is taken by fitting the data before and after the offline cuts are made. The final branching fraction is given by (2.2).

$$\frac{BF_{phh}}{BF_{pK\pi}} = \frac{N_{phh_{measured}}}{N_{pK\pi_{measured}}} \times \frac{\epsilon_{trig|pK\pi}}{\epsilon_{trig|phh}} \times \frac{\epsilon_{strip|pK\pi}}{\epsilon_{strip|phh}} \times \frac{\epsilon_{offline|pK\pi}}{\epsilon_{offline|phh}} \times \frac{\epsilon_{PID|pK\pi}}{\epsilon_{PID|phh}} \tag{2.2}$$

Using information from the RICH, variables are constructed which give the difference of log likelihoods of a charged track matching each particle identification hypothesis. These variables are used as discriminants in the trigger and stripping, but are poorly modelled in MC. To account for this a data-driven calibration is performed and the PID efficiency is entirely factored out from the other efficiencies. The assumption is made that a suite of kinematic variables can fully characterise the PID variable response. Modes which can be cleanly reconstructed without the use of PID cuts in the trigger or stripping are used to acquire samples of protons, kaons and pions without any cuts on the PID variables. These are used to construct efficiency histograms of the cuts used on PID variables on our signal samples in the kinematic bins and each signal track is then assigned an efficiency weight corresponding to the efficiency of the kinematic bin it falls in.

2.2.3 Systematic Uncertainties

Thus far the dominant systematic uncertainty in the analysis is that associated with the PID calibration. This arises from two sources. The first is due to the statistical uncertainty arising from the

finite size of the calibration sample. The second arises as a consequence of the finite bin width of the efficiency histograms. The PID response of a track varies by a finite amount across individual kinematic bins, which are assigned an average PID response based on the average PID response of calibration mode tracks falling in that bin. The signal tracks have kinematic distributions which are different to those of the calibration sample, so the average PID efficiency of the signal tracks within a given bin will be different to the average of the calibration tracks. This causes a bias in the calibration which must be evaluated.

This is done by constructing efficiency histograms using calibration MC, then using a source of signal MC without PID response cuts in the calibration procedure. As there are no cuts on the signal MC the true efficiency of a given PID response cut can be attained and compared to the calculated value yielded by the calibration procedure. As the discrepancy between these two values varies depending on the PID response cut used, the discrepancy is calculated over a range of PID response cuts around the value used in the selection. The maximum discrepancy is quoted as the systematic of the calibration procedure, which in this analysis is 3%.

There are a number of other sources of systematic uncertainty which are currently being evaluated. These are associated with the fit model and the agreement between data and MC, but are expected to be small compared to the PID calibration systematic.

2.2.4 Current Results and Future Work

Mode	Stream	$\mathcal{BF}$ Relative to $\Lambda_c^+ \to p^+K^-\pi^+$ [%]	Discrepancy between Prompt/SL
$\Lambda_c^+ \to p^+\pi^-\pi^+$	Prompt	$6.917 \pm 0.266(stat) \pm 0.207(syst)$	1.1σ
	SL	$6.532 \pm 0.075(stat) \pm 0.195(syst)$	
$\Lambda_c^+ \to p^+K^-K^+$	Prompt	$2.055 \pm 0.092(stat) \pm 0.061(syst)$	4.1σ
	SL	$1.606 \pm 0.028(stat) \pm 0.048(syst)$	
$\Lambda_c^+ \to p^+(\phi \to K^-K^+)$	Prompt	$0.973 \pm 0.058(stat) \pm 0.029(syst)$	1.7σ
	SL	$0.858 \pm 0.018(stat) \pm 0.025(syst)$	

Table 2: Current results for the relative branching fraction measurements.

The current measurements are given in Table 2. There exists agreement between the measurements of $\Lambda_c^+ \to p^+\pi^-\pi^+$. The large discrepancy between prompt and semileptonic in the $\Lambda_c^+ \to p^+K^-K^+$ measurement is highly reduced in the $\Lambda_c^+ \to p^+(\phi \to K^-K^+)$ measurement. This indicates that variations in acceptance across those variables which characterise the resonant structure of the decay are at least partially responsible for the discrepancy in $\Lambda_c^+ \to p^+K^-K^+$. These resonance variables are not modelled in the prompt MC and not modelled well in the semileptonic MC. Work re-weighting our efficiencies to account for this is currently underway. When agreement between the prompt and semileptonic is established the doubly cabibbo suppressed $\Lambda_c^+ \to p^+\pi^-K^+$ mode will be unblinded and the results written up in a paper for external publication.

3 Future Work and Thesis

3.1 Future Work

Work on the measurements of Λ_c^+ $\mathcal{BF}$s is nearing completion. Work on investigating VELO weak mode effects is still in progress and requires further investigation of the effects of the constraints on the alignment. When these effects are investigated, and if an effective way of minimising weak mode effects can be established, the results will be written up in an internal LHCb note. The author has also performed some early work on another LHCb analysis, the search for the doubly charmed baryon Ξ_{cc}^+, which has been observed by the SELEX collaboration [3] but not been observed by subsequent searches at b-factories (see e.g. [4],[5]). Upon completion of the $\Lambda_c^+ \to p^+h^-h^+$ $\mathcal{BF}$ analysis the author will resume this work.

3.2 Plan for Thesis

Work on the thesis will begin upon the author's return to Glasgow at the end of September. The chapters of the thesis shall be:

1. An introduction to the thesis briefly outlining the structure.
2. A chapter on the theory behind the standard model of particle physics, explaining the concepts of particle physics relevant to the author's work in charmed baryon spectroscopy (e.g. Cabibbo suppression and resonances in baryon decays).
3. A chapter detailing the LHCb experiment and detector. Features of the detector, trigger and data processing relevant to the author's work will be detailed.
4. A chapter on the author's work on VELO weak modes, detailing the MC study of weak mode effects and the techniques/constraints which were investigated in an attempt to suppress them.
5. A chapter on the analysis of $\Lambda_c^+ \to p^+h^-h^+$ $\mathcal{BF}$s, detailing the analysis in full and outlining the final results.
6. A chapter detailing the author's work on searches for doubly charmed baryons.
7. A chapter concluding the thesis.

GANTT CHART GOES HERE

References

[1] K. Nakamura et al. (Particle Data Group), JPG 37, 075021 (2010).

[2] Gersabeck M, 2009, 'Alignment of the LHCb Vertex Locator and Lifetime Measurements of Two-Body Hadronic Final States' PhD Thesis, Univ. of Glasgow.

[3] Mattson, M. et al, 'First Observation of the Doubly Charmed Baryon Xi_{cc}^{+}' Phys.Rev.Lett. 89:112001, 2002.

[4] B. Aubert, et al, 'Search for Doubly Charmed Baryons Ξ_{cc}^{+} and Ξ_{cc}^{++} in BABAR' Phys.Rev.D 74:011103,2006

[5] R.Chistov, et al, 'Observation of New States Decaying into $\Lambda_c^+ K^- \pi^+$ and $\Lambda_c^+ K_S^0 \pi^-$' Phys.Rev.Lett. 97:162001,2006